

## $\Delta$ excitation and exchange corrections for $NN$ bremsstrahlung

M. Jetter and H. W. Fearing

*TRIUMF, 4004 Wesbrook Mall, Vancouver, British Columbia, Canada V6T 2A3*

(Received 21 October 1994)

The role of the relativistic amplitudes for a number of  $O(k)$  processes usually neglected in potential model calculations of  $NN$  bremsstrahlung is investigated. In particular, we consider the  $\Delta$  excitation pole contributions related to the one-pion and one-rho exchange and in addition include the exchange contributions induced by the radiative  $\omega, \rho \rightarrow \pi\gamma$  decays. The contributions are calculated from relativistic Born amplitudes fitted to  $\Delta$  production and absorption data in the energy range up to 1 GeV and then used to supplement potential model and soft photon calculations for nucleon-nucleon bremsstrahlung. The effects on  $NN\gamma$  observables, although moderate in general, are found to be important in some kinematic domains.

PACS number(s): 13.75.Cs, 25.20.-x, 25.40.-h

### I. INTRODUCTION

Nucleon-nucleon bremsstrahlung has been extensively investigated both experimentally and theoretically during the past 30 years. For  $pp \rightarrow pp\gamma$  the experimental data available cover an energy domain between 42 MeV [1] and 730 MeV [2], the most recent results being obtained at incident proton energies around the pion production threshold [3-5]. Up to the pion production threshold, the  $NN\gamma$  potential model using realistic  $NN$  potentials for the description of the nuclear force plus first order approximation for the electromagnetic interaction gives the most successful description.

A comparison of different  $NN$  interactions yields widely equivalent  $NN\gamma$  results in the whole kinematic range [6], so that bremsstrahlung provides a sensitive test for the dynamical model used to describe the photon emission. In the framework of the potential model, however, there is little controversy about the basic features and the correction terms to be used. In particular, relativistic spin corrections as derived in [7,8] and rescattering contributions [9] are used in the most recent analyses [6,10]; see also [11,12]. Moreover, the role of Coulomb corrections in  $pp\gamma$  [13] and exchange currents in the  $np\gamma$  cross section have been discussed [9,14].

The main theoretical problems left are presumably related to shortcomings in principle of the potential model description. For example, Lorentz invariance can only be accounted for approximately by a covariant treatment of the kinematic transformations, inclusion of higher order terms in  $(p/m)$  in the electromagnetic operator (relativistic spin corrections), and an appropriate description of the  $NN$  interaction. Further common features of existing potential model calculations are the absence of dynamical baryon resonances and the neglect of two-body currents beyond the  $O(k^0)$  terms given by the soft photon approximation (SPA).

The role of  $\Delta$  excitation was studied in the 1970s in two different approaches. The authors of [15] used a dispersion analysis in order to correct the one-pion exchange (OPE) neutron-proton electromagnetic current. The ef-

fect of the  $\Delta$  resonance on the  $np\gamma$  cross section at 200 MeV turned out to be small. In [16] and [17], the  $\Delta$ -excitation part of the  $pp\gamma$  amplitude was derived from phenomenological Lagrangians and combined with soft photon or one-boson exchange (OBE) Born calculations for the radiative background.

A more sophisticated potential approach including effects of the  $\Delta$ , based on a coupled channels calculation of the half off-shell  $NN$  and  $N\Delta T$  matrices together with a phenomenological  $N\Delta\gamma$  vertex, has been published recently [18,19]. In contrast to the  $np\gamma$  results of [15], the authors find an appreciable  $\Delta$  contribution to the 280 MeV  $pp\gamma$  observables.

For higher energies where the potential model is inappropriate, the closely related problem of dilepton production has recently been studied in the framework of an effective one-boson exchange plus  $\Delta$ -excitation Born approximation [20].

As mentioned above, a rigorous derivation of induced two-body currents is not possible to all orders. The reason is that, unlike, e.g., for a one-pion exchange potential [21], the gauge-invariant replacement  $V_N(\vec{p}) \rightarrow V_N(\vec{p} - e\vec{A})$  in the argument of a general  $NN$  potential  $V_N$  [9,14] leads to a unique expression for the induced current only in the SPA. To this order, the induced current approximates contributions due to the exchange of charged mesons and vanishes for  $pp\gamma$ . The radiative decay processes we are considering here are thus not accounted for in the conventional potential model. Apart from an early estimate of the small  $\rho^0$  contribution [22], only the radiative  $\omega \rightarrow \pi^0\gamma$  decay for  $pp\gamma$  has been considered as an example of such an  $O(k)$  internal radiation process [23].

The purpose of the present work is to provide an estimate of the role of baryon resonances and internal radiation processes reliable up to photon energies of about 300 MeV corresponding to the highest photon energy possible in the 730 MeV  $pp\gamma$  experiment of [2]. From a comparison with recent analyses of pion photoproduction [24], we expect the  $\Delta(1232)$  resonance and the radiative decay of the  $\omega$  and  $\rho$  to be the leading corrections.

A coupled channels calculation for the  $NN-N\Delta$  system omitting the contribution of the  $\Delta\Delta$  states (as, for example, in [25]) typically consists in solving a set of integral equations which represent one of the three-dimensional reductions of the Bethe-Salpeter equation

$$T_{NN} = V_{NN} + V_{NN}G_N T_{NN} + V_{N\Delta}G_\Delta T_{\Delta N}, \quad (1.1)$$

$$T_{\Delta N} = V_{\Delta N} + V_{\Delta N}G_N T_{NN} + V_{\Delta\Delta}G_\Delta T_{\Delta N}. \quad (1.2)$$

Inclusion of the  $\Delta$  thus modifies the  $NN$  amplitude  $T_{NN}$  and yields an additional amplitude  $T_{\Delta N}$ . The pure  $NN$  interaction below the pion production threshold is known to be well described by phenomenological and/or meson theoretic potentials so that we feel safe identifying  $T_{NN}$  of Eq. (1.1) with a pure  $NN$ - $T$  matrix calculated from a realistic nuclear potential, in effect absorbing the  $V_{N\Delta}G_\Delta T_{\Delta N}$  piece. By then adding the  $\Delta$ -excitation Born terms, we basically neglect the modifications of the amplitude  $T_{\Delta N}$  [Eq. (1.2)] induced by the iterative terms. Empirically, i.e., from a comparison of the Born amplitude  $V_{\Delta N}$  with coupled channels  $\Delta$ -absorption predictions for laboratory energies of 50–300 MeV [25], and experimental  $\Delta$ -production data at 800 MeV [26] and 970 MeV [27], it turns out that the effect of the iteration can be simulated by a simple energy-dependent rescaling of the Born amplitude in a good approximation. We are then left basically with two sources of possible errors: (1) We superpose a (necessarily real and therefore not unitary) Born amplitude with the iterated potential model and SPA amplitudes. (2) A consistent inclusion of  $\Delta$  channels, while leaving the phase shifts unchanged, might lead to modifications of the off-shell behavior of the  $NN$  interaction (and of the  $N\Delta$  interaction via the iterative terms) even below the pion production threshold. Both effects should be small as long as the  $\Delta$  channel is small compared to the leading  $NN$  amplitude which is the case in all geometries displayed in this work. Moreover, as will be shown below for the 280 MeV  $pp\gamma$  cross section, the  $\Delta$  contribution is suppressed for geometries with extremely large photon momentum (and thus off-shell signature) due to a small four-momentum transfer at the  $\pi N\Delta/\rho n\Delta$  vertices.

Our approach for the  $\Delta$  is thus complementary to a

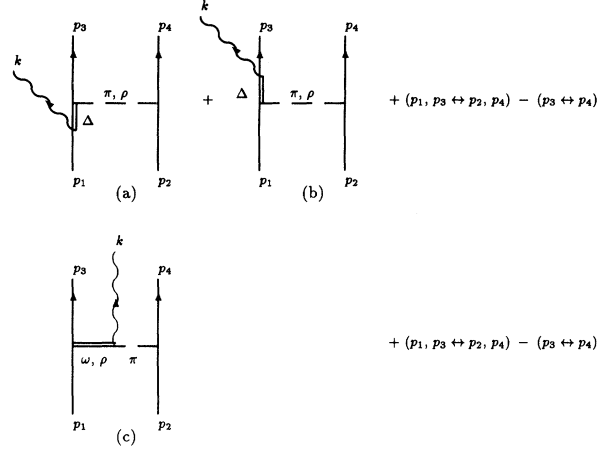


FIG. 1.  $\Delta$  excitation and internal radiation processes considered in this paper.

full coupled channels calculation [18] which systematically avoids the shortcomings mentioned above but cannot be extended easily to processes such as the internal radiative decays and ultimately has to rely on an approximate treatment of relativistic effects.

In the following two sections, a description of the model together with a discussion of the parameters will be given. Results for  $pp\gamma$  and  $np\gamma$  are presented in Sec. IV. We have taken care to test thoroughly the influence of the experimental and theoretical uncertainties for the various ingredients of the amplitude that cannot be fixed to accurate data. The results might be useful to estimate the reliability not only of this but of any comparable calculation.

## II. INCLUSION OF THE $\Delta$

For the derivation of the  $\Delta$ -excitation terms depicted in Fig. 1 we start from the interaction Lagrangians for the isovector mesons  $\pi$  and  $\rho$  (see [28]) in the notation of [29]:

$$\mathcal{L}_{\pi NN} = -ig_{\pi NN}\bar{\psi}\gamma_5\vec{T}\psi\vec{\pi}, \quad (2.1)$$

$$\mathcal{L}_{\rho NN} = -g_{\rho NN}\left(\bar{\psi}\gamma^\mu\vec{T}\psi\vec{\rho}_\mu + \frac{\kappa_\rho}{4m_N}\bar{\psi}\sigma^{\mu\nu}\vec{T}\psi(\partial_\mu\vec{\rho}_\nu - \partial_\nu\vec{\rho}_\mu)\right), \quad (2.2)$$

$$\mathcal{L}_{\pi N\Delta} = -\frac{g_{\pi N\Delta}}{m_\pi}\bar{\psi}\vec{T}\psi^\mu\partial_\mu\vec{\pi} + \text{H.c.}, \quad (2.3)$$

$$\mathcal{L}_{\rho N\Delta} = i\frac{g_{\rho N\Delta}}{m_\rho}\bar{\psi}\gamma^5\gamma^\mu\vec{T}\psi^\nu(\partial_\mu\vec{\rho}_\nu - \partial_\nu\vec{\rho}_\mu) + \text{H.c.}, \quad (2.4)$$

where  $\psi_\Delta$  is the spin-3/2 Rarita-Schwinger field and  $\vec{T}$  stands for the isospin operator for the transition of an isospin-1/2 and isospin-1 to an isospin-3/2 particle [28]. We have used the pseudoscalar  $\pi NN$  coupling for convenience. As the  $\pi NN$  vertices in our calculations involve only on-shell nucleons, pseudovector coupling for the pion instead of Eq. (2.1) would not change any of our results. From Eqs. (2.1)–(2.4), the vertex functions read

$$\begin{aligned} \Lambda_{\pi NN} &= g_{\pi NN}\gamma_5, & \Lambda_{\rho NN}^\mu(q) &= -ig_{\rho NN}\left(\gamma^\mu - \frac{\kappa_\rho}{2m_N}i\sigma^{\mu\nu}q_\nu\right), \\ \Lambda_{\pi N\Delta}^\mu(q) &= \frac{g_{\pi N\Delta}}{m_\pi}q^\mu, & \Lambda_{\rho N\Delta}^{\mu\nu}(q) &= i\frac{g_{\rho N\Delta}}{m_\rho}(i\hat{g}^{\mu\nu} - \gamma^\mu q^\nu)\gamma_5, \end{aligned} \quad (2.5)$$

and one derives the transition amplitudes for diagram (a) in Fig. 1 [17],

$$T^{(1)}(p_1, p_2; p_3, p_4) = \bar{u}(p_3)\Lambda_{\pi N\Delta}^\nu(q)P_{\nu\sigma}^\Delta(p_1 - k)\epsilon_\mu\Gamma_{\gamma N\Delta}^{\mu\sigma}(k, p_1 - k)u(p_1)P^\pi(q)\bar{u}(p_4)\Lambda_{\pi NN}u(p_2) \\ + \bar{u}(p_3)\Lambda_{\rho N\Delta}^{\lambda\nu}(q)P_{\nu\sigma}^\Delta(p_1 - k)\epsilon_\mu\Gamma_{\gamma N\Delta}^{\mu\sigma}(k, p_1 - k)u(p_1)P_{\lambda\tau}^\rho(q)\bar{u}(p_4)\Lambda_{\rho NN}^\tau u(p_2), \quad (2.6)$$

and equivalently for diagram (b),

$$T^{(2)}(p_1, p_2; p_3, p_4) = \bar{u}(p_3)\epsilon_\mu\tilde{\Gamma}_{\gamma N\Delta}^{\mu\sigma}(k, p_3 + k)P_{\sigma\nu}^\Delta(p_3 + k)\tilde{\Lambda}_{\pi N\Delta}^\nu(q)u(p_1)P^\pi(q)\bar{u}(p_4)\Lambda_{\pi NN}u(p_2) \\ + \bar{u}(p_3)\epsilon_\mu\tilde{\Gamma}_{\gamma N\Delta}^{\mu\sigma}(k, p_3 + k)P_{\sigma\nu}^\Delta(p_3 + k)\tilde{\Lambda}_{\rho N\Delta}^{\lambda\nu}(q)u(p_1)P_{\lambda\tau}^\rho(q)\bar{u}(p_4)\Lambda_{\rho NN}^\tau u(p_2). \quad (2.7)$$

Here, the energies and momenta are constrained according to  $p_1 + p_2 = p_3 + p_4 + k$ ,  $q = p_4 - p_2$  is the four momentum transferred by the meson,  $\epsilon_\mu$  the photon unit polarization vector,  $u, \bar{u}$  denote free nucleon Dirac spinors, and  $P$  the appropriate propagators for the mesons and the  $\Delta$ . With the tilde in Eq. (2.7) we indicate that the vertex function has to be taken from the Hermitian conjugate of the corresponding Lagrangian.

Associated with Eqs. (2.6) and (2.7) are isospin factors, e.g., in the case of proton-proton bremsstrahlung:

$$\langle\chi_p | T_3 | \chi_{\Delta^+}\rangle\langle\chi_{\Delta^+} | T_3 | \chi_p\rangle\langle\chi_p | \tau_3 | \chi_p\rangle = \frac{2}{3}.$$

The full  $\Delta$ -excitation amplitude including the isospin factors and a relative minus for graphs involving interchange of the final state particles is then

$$T_\Delta^{pp\gamma} = \frac{2}{3} \sum_{i=1}^2 \left\{ T^{(i)}(p_1, p_2; p_3, p_4) + T^{(i)}(p_2, p_1; p_4, p_3) - [T^{(i)}(p_1, p_2; p_4, p_3) + T^{(i)}(p_2, p_1; p_3, p_4)] \right\} \\ T_\Delta^{np\gamma} = \frac{2}{3} \sum_{i=1}^2 \left\{ [-T^{(i)}(p_1, p_2; p_3, p_4) + T^{(i)}(p_2, p_1; p_4, p_3)] + (-1)^{(i)}[-T^{(i)}(p_1, p_2; p_4, p_3) + T^{(i)}(p_2, p_1; p_3, p_4)] \right\}. \quad (2.8)$$

For the electromagnetic  $N\Delta$  current of diagram (a) we use the parametrization [33]

$$\Gamma_{\gamma N\Delta}^{\mu\nu}(k, p) = -ie \left\{ \frac{G_1}{m_N} (\gamma^\mu k^\nu - k g^{\mu\nu}) + \frac{G_2}{m_N^2} (p^\mu k^\nu - k \cdot p g^{\mu\nu}) \right\} \gamma_5. \quad (2.9)$$

$\tilde{\Gamma}_{\gamma N\Delta}(k, p)$  is equal to  $\Gamma_{\gamma N\Delta}(k, p)$  up to a relative minus sign in the term proportional to  $G_1$ . The couplings  $G_1$  and  $G_2$  are experimentally determined by a fit to the  $M1^+/E1^+$  multipole pion-photoproduction cross section. This has often been done simultaneously with the off-shell parameters  $Z_\pi$  and  $Z_\gamma$  discussed below, so that the different sets of coupling constants quoted have to be interpreted carefully. However, according to Davidson *et al.*, [30],  $G_1, G_2$ , and the  $Z$  parameters are only weakly correlated in a multipole analysis so that all the coupling vertices  $\Gamma_{\gamma N\Delta}$  used in the literature should be equivalent to a good approximation. Values for the couplings range from  $G_1 = 1.90, G_2 = -0.75$  [31],  $G_1 = 2.40, G_2 = -1.43$  [32], to  $G_1 = 2.51, G_2 = -1.62$  [18,33], a recently quoted set being  $G_1 = 2.208, G_2 = -0.556$  [24]. A simple vector dominance model yields  $G_1 = \sqrt{3} \frac{m_N}{m_\rho} \frac{g_{\rho N\Delta}}{g_{\rho NN}}$ ,  $G_2 = 0$ , i.e.,  $G_1 = 1.90$  (1.49) with the rho couplings of model A (B) defined below. Theoretical predictions of the electromagnetic  $\Delta$  coupling  $G_1$  based on quark models or the Skyrme model typically fall short of the experimental value by (20–30)% [34,35].

The choice of the  $\Delta$  propagator requires some caution. In [17], the Rarita-Schwinger form

$$P_\Delta^{\mu\nu}(p) = \frac{\not{p} + m_\Delta}{p^2 - m_\Delta^2 + i\Gamma m_\Delta} \left( g^{\mu\nu} - \frac{1}{3} \gamma^\mu \gamma^\nu - \frac{2}{3} \frac{p^\mu p^\nu}{m_\Delta^2} - \frac{\gamma^\mu p^\nu - p^\mu \gamma^\nu}{3m_\Delta^2} \right) \quad (2.10)$$

is used where the replacement  $m_\Delta \rightarrow m_\Delta - i\Gamma/2$  is made in order to account for inelasticities due to pion production. As we wish to use  $P_\Delta$  in the far-off-resonance region ( $p^2 \ll m_\Delta^2$ ), we have to take the energy dependence of the width  $\Gamma \rightarrow \Gamma(q)$  into account. For our purpose, we rely on the Bransden-Moorhouse parametrization of [36] requiring  $\Gamma$  to vanish below the pion production threshold:

$$\Gamma(q_{\pi N}) = 0, \quad q_{\pi N}^2 \leq 0, \\ \Gamma(q_{\pi N}) = 2\gamma(q_{\pi N} R/m_\pi)^3 / (1 + (q_{\pi N} R/m_\pi)^2), \\ q_{\pi N}^2 > 0. \quad (2.11)$$

Here,  $q_{\pi N}$  denotes the maximum momentum in the  $\pi N$  subsystem of the process  $NN \rightarrow NN\pi$ :

$$q_{\pi N}^2 = (s_{\pi N} - (m_\pi - m_N)^2)(s_{\pi N} - (m_\pi + m_N)^2) / 4s_{\pi N}, \\ s_{\pi N} = (\sqrt{s} - m_N)^2, \quad (2.12)$$

$\sqrt{s}$  is the invariant energy in the  $NN$  system, and  $R, \gamma$  are adjustable parameters. Values of  $\gamma = 0.71$  MeV,  $R = 0.81$  lead to a resonance width  $\Gamma = 120$  MeV at  $\sqrt{s_{\pi N}} = 1236$  MeV [36]. This value might be slightly modified by a variation of  $\gamma$ .

The  $\Delta$  propagator has been derived more consistently

by solving the Dyson equation for the (energy-dependent) self-energy  $\Sigma_\Delta$  [37,25]. If the negative energy part of the  $\Delta$  propagator is omitted and its spin dependence is ignored, this leads to a well-determined imaginary part  $\text{Im}(\Sigma_\Delta)$ . The energy dependence of the real part  $\text{Re}(\Sigma_\Delta)$  off resonance is more strongly affected by the cutoff procedure used in the calculation. For this reason [and because we want to keep the full Rarita-Schwinger propagator (2.10)], a detailed comparison of the Bransden-Moorhouse parametrization with the result of [25] is difficult. Above threshold it has been shown [37] that the parametrization (2.11) agrees with the experimental  $\delta_{33}$  phase as well as a  $\Delta$  self-energy calculation (the value for the propagator at resonance is actually exact by construction). At threshold  $q_{\pi N} = 0$ , the values for  $\text{Re}(\Sigma_\Delta)$  plotted in [25] effectively increase  $m_\Delta$  by a few percent, which would slightly attenuate the  $\Delta$  contribution.

$NN$ - $N\Delta$  potential models differ in the choice of the  $\Delta$ -coupling constants as well as in the definition of the

meson propagators and vertex form factors. We use these models as a starting point for our calculation defining the  $\Delta$ -excitation amplitude up to a normalization. In a reliable calculation, the final results should not depend too much on the underlying parameter sets provided they agree comparably well with the empirical  $NN$  data. We therefore compare two different recent coupled channels models: The OBE model of [25], denoted as model A, and a coupled channels version of the Bonn potential (model I of [28], p. 353), denoted as model B. For model A, we use the meson propagators

$$P^{(\pi)} = \frac{i}{q^2 - m_\pi^2}, \quad P_{\mu\nu}^{(\rho)} = i \frac{-g_{\mu\nu} + q_\mu q_\nu / m_\rho^2}{q^2 - m_\rho^2}. \quad (2.13)$$

The second term in  $P^{(\rho)}$  drops out in the calculations of this and the following section. The propagators of model B take the mass difference between the nucleon and the  $\Delta$  into account:

$$P^{(\pi)} = -i \left\{ \frac{1}{2\omega_\pi^2} + \frac{1}{2\omega_\pi(m_\Delta - m_N + \omega_\pi)} \right\}, \quad \omega_\pi \equiv \sqrt{m_\pi^2 - q^2},$$

$$P_{\mu\nu}^{(\rho)} = i g_{\mu\nu} \left\{ \frac{1}{2\omega_\rho} + \frac{1}{2\omega_\rho(m_\Delta - m_N + \omega_\rho)} \right\}. \quad (2.14)$$

In writing down the Lorentz-invariant propagators (2.13) and (2.14) we have dropped the static approximation  $q^2 \rightarrow -\vec{q}^2$  of the potential models A and B. As we are far from the pole in all our geometries and rescale our final amplitudes this has very little effect on the end results.

For the calculations using model A, each  $NN\pi/NN\rho$  vertex is multiplied by a monopole cutoff  $\Lambda_{\pi/\rho}^2/(\Lambda_{\pi/\rho}^2 - q^2)$  and a dipole cutoff  $[\Lambda_{\Delta\pi/\rho}^2/(\Lambda_{\Delta\pi/\rho}^2 - q^2)]^2$  applies at the  $N\Delta\pi/\rho$  vertices. Here again, we use Lorentz invariant instead of static expressions. For model B, both the  $NN$  and  $N\Delta$  vertices are regularized by cutoffs  $[(\Lambda^2 - m_{\pi/\rho}^2)/(\Lambda^2 - q^2)]^n$  where  $n = 1, 2$  for  $\pi, \rho$  exchange, respectively.

In general, the relativistic off-shell  $\Delta$  particle is allowed to propagate with both spin 3/2 and spin 1/2. This extra freedom is reflected by additional off-shell terms in the interaction Lagrangians; the more general chiral  $\pi N\Delta$ -vertex functions corresponding to the propagator (2.10) read [38,39]

$$\Lambda_{\pi N\Delta}^\mu = \frac{g_{\pi N\Delta}}{m_\pi} \Theta^{\mu\nu}(Z_\pi) q_\nu, \quad \Lambda_{\rho N\Delta}^{\mu\nu} = i \frac{g_{\rho N\Delta}}{m_\rho} (\not{A} \Theta^{\mu\nu} - \gamma^\mu q_\alpha \Theta^{\alpha\nu}) \gamma_5,$$

$$\Theta^{\mu\nu}(Z_{\pi/\rho}) = g^{\mu\nu} - (Z_{\pi/\rho} + \frac{1}{2}) \gamma^\mu \gamma^\nu. \quad (2.15)$$

A generalization similar to  $\Lambda_{\rho N\Delta}$  (with parameter  $Z_\gamma$ ) applies for the (leading)  $G_1$  term of Eq. (2.9). The  $Z$  parameters are not well determined either theoretically or experimentally. Whereas the simple coupling scheme corresponding to  $Z = -1/2$  is generally preferred in potential models, Olssen and Osypowski [39] find experimental values of  $Z_\pi = 0 \pm 1/4$ ,  $Z_\gamma = 1/4 \pm 1/4$ . In the comprehensive multipole study already quoted by Davidson *et al.* [30], a best fit is obtained with  $Z_\pi = -0.24$ ,  $Z_\gamma = -0.53$ , but with a rather large dependence on details of the fit and in particular the size of the  $t$ -channel  $\omega$ -decay diagrams. This latter study seems to rule out the field theoretical prediction by Nath and Bhattacharyya [40] that, for pointlike spin-3/2 particles, both off-shell parameters are constrained to values of 1/2, whereas  $G_2 = 0$ . On the other hand, it has been shown earlier [41] that there is no firm basis for Peccei's choice of  $Z_\pi = -1/4$  [45,24].

Note that the off-shell parameters do not affect a coupled channels calculation at the OBE level but directly enter the Born amplitude for the bremsstrahlung process where the  $\Delta$  is off shell. We therefore rely on the parameters of Table I as fixed by  $NN$  data (to all orders

TABLE I. Meson parameter of models A and B. For the definition of form factors, propagators, etc., see text.

	Model A [25]		Model B [28]	
	$\frac{g^2}{4\pi}$	$\Lambda$ [MeV]	$\frac{g^2}{4\pi}$	$\Lambda$ [MeV]
$NN\pi$	14.16	1140	14.4	1800
$NN\rho$	0.43	1140	0.7	2200
	$\kappa = 5.1$		$\kappa = 6.1$	
$N\Delta\pi$	0.35	910	0.35	920
$N\Delta\rho$	4.0	910	19.0	1140

of a coupled channels calculation) with the simple choice  $Z = -1/2$  but check the sensitivity of our results to a variation of  $Z$ .

This completes the necessary ingredients for the  $\Delta$ -excitation part of the bremsstrahlung amplitude (2.8). With the definitions of this section we have tried to incorporate as much as possible of the experimental information on the  $N\Delta$ -excitation channels in the  $NN$  interaction which have become available since the earlier Born calculations [17,16]. On the other hand, the rel-

ativistic approach allows us—in contrast to a pure potential model calculation [18]—to extend the analysis to energies far beyond the pion production threshold.

### III. INCLUSION OF THE RADIATIVE $\omega/\rho$ DECAY

We write the Lagrangian for the coupling of the  $\omega$  meson to the nucleons in analogy to Eq. (2.2):

$$\mathcal{L}_{\omega NN} = -g_{\omega} \left( \bar{\psi} \gamma^{\mu} \psi \omega_{\mu} + \frac{\kappa_{\omega}}{4m_N} \bar{\psi} \sigma^{\mu\nu} \psi (\partial_{\mu} \omega_{\nu} - \partial_{\nu} \omega_{\mu}) \right), \quad (3.1)$$

and parametrize the radiative decay vertices as in [24],

$$\mathcal{L}_{\omega\pi\gamma} = g_{\omega\pi\gamma} \varepsilon_{\nu\rho\sigma\delta} (\partial^{\sigma} A_{\gamma}^{\rho}) (\partial^{\nu} \pi^0) \omega^{\delta} \rightarrow \Lambda_{\rho\delta}^{\omega\pi\gamma}(k, q) = -i g_{\omega\pi\gamma} \varepsilon_{\nu\rho\sigma\delta} k^{\sigma} q^{\nu}, \quad (3.2)$$

$$\mathcal{L}_{\rho^i\pi\gamma} = g_{\rho^i\pi\gamma} \varepsilon_{\nu\rho\sigma\delta} (\partial^{\sigma} A_{\gamma}^{\rho}) (\partial^{\nu} \pi^i) \rho^{i,\delta}, \quad i = 0, +, -. \quad (3.3)$$

With the meson propagators as in (2.13) and a vertex function  $\Lambda_{\omega NN}^{\mu}$  as in Eq. (2.5) this yields for the diagram (c) of Fig. 1

$$T_{\omega\pi\gamma}^{(c)}(p_1, p_2; p_3, p_4) = \bar{u}(p_3) \Lambda_{\mu}^{\omega NN}(p_3 - p_1) u(p_1) P_{(\omega)}^{\mu\delta}(p_3 - p_1) \Lambda_{\delta\rho}^{\omega\pi\gamma}(k, p_4 - p_2) \epsilon_{\gamma}^{\rho} \\ \times P_{(\pi)}(p_4 - p_2) \bar{u}(p_4) \Lambda^{\pi NN} u(p_2), \quad (3.4)$$

and consequently [see Eq. (2.8)]

$$T_{\omega\pi\gamma}^{pp\gamma} = T(p_1, p_2; p_3, p_4) + T(p_2, p_1; p_4, p_3) - [T(p_1, p_2; p_4, p_3) + T(p_2, p_1; p_3, p_4)], \\ T_{\omega\pi\gamma}^{n\pi\gamma} = T(p_1, p_2; p_3, p_4) - T(p_2, p_1; p_4, p_3). \quad (3.5)$$

The  $\rho$  decay amplitudes are obtained from  $T_{\omega\pi\gamma}$  by interchange of the masses and coupling constants and multiplication with the isospin operator  $\vec{\tau}_1 \cdot \vec{\tau}_2$ . The matrix elements of this operator yields factors of 1 and 0 for the neutral and charged pion decay amplitude in  $pp\gamma$ . For  $n\pi\gamma$  the corresponding values are  $-1$  and  $2$ .

The coupling constants  $g_{\omega\pi\gamma}$  and  $g_{\rho\pi\gamma}$  are determined from the experimental decay widths of the vector mesons [42]:

$$\Gamma(\omega/\rho \rightarrow \pi\gamma) = \frac{g_{\omega/\rho\pi\gamma}^2 (m_{\omega/\rho}^2 - m_{\pi}^2)^3}{96\pi m_{\omega/\rho}^3} = \begin{cases} 716 \pm 75 \text{ keV} & \text{for } \omega, \\ 121 \pm 31 \text{ keV} & \text{for } \rho^0, \\ 68 \pm 7 \text{ keV} & \text{for } \rho^{\pm}. \end{cases} \quad (3.6)$$

This leads to the numerical values

$$\frac{g_{\omega\pi\gamma}^2}{4\pi} = 0.715 \times 10^{-3} m_{\pi}^{-2}, \quad \frac{g_{\rho^0\pi\gamma}^2}{4\pi} = 0.125 \times 10^{-3} m_{\pi}^{-2}, \quad \frac{g_{\rho^{\pm}\pi\gamma}^2}{4\pi} = 0.070 \times 10^{-3} m_{\pi}^{-2}. \quad (3.7)$$

For the remaining coupling constants and cutoffs, we again follow the rationale of the previous section and use a complete set that has been successfully tested in pion photoproduction [24]. Thus we put

$$\frac{g_{\rho}^2}{4\pi} = 0.563, \quad \kappa_{\rho} = 3.71, \quad \frac{g_{\omega}^2}{4\pi} = 5.07, \quad \kappa_{\omega} = -0.12. \quad (3.8)$$

These values are in agreement with the quark model and the vector dominance assumption. All form factors in this section are set to 1; the pion couplings are taken from Table I. Note that a measurement of the vector meson radiative decay contributions in the pion-

photoproduction process determines the product of the couplings in Eqs. (3.7) and (3.8). With the well-known empirical value of  $g_{\pi}$ , the amplitude (3.4) is therefore essentially fixed.

### IV. RESULTS

As mentioned earlier, the amplitudes (2.8) and (3.4) must be divided by an energy-dependent scaling factor  $g(T_{\text{lab}})$  in order to compensate for neglecting higher order terms in the Born series. From a comparison of our Born results using model A with the total  $\Delta$ -absorption cross sections of [25] calculated in the iterated coupled

channels model, one finds a factor  $g = 1.65$  at laboratory energies below 300 MeV. A calculation of the total  $\Delta$ -production cross section and comparison with the experimental data at 800 MeV [26] and 970 MeV [27] suggests a weak energy dependence of  $g$  so that  $g(730 \text{ MeV}) = 1.4$ . The latter value is in close agreement with the result of [20]. As we have to compensate also for the change from static to Lorentz-invariant propagators in Eqs. (2.13) and (2.14), we use  $g(280 \text{ MeV}) = 1.95$  and  $g(730 \text{ MeV}) = 1.65$ , respectively.

If we suppose the higher order corrections to be of equal importance for both models A and B and for the  $\omega/\rho$  decay amplitudes for which no experimental comparison could be made, the model is completely determined with the empirical values of  $g(T_{\text{lab}})$  found above. The rescaled amplitudes (2.8) and (3.4) can thus be coherently added to the corresponding transition matrices of the potential model [6] and the soft photon approximation [43,44] so that the effects upon both cross sections and spin observables can be studied. The relevant formula for the observables considered can be found in the literature [8,17]. For the potential model calculations we shall focus on the domain around the pion production threshold where both correction effects should be maximum; the soft photon model will be used to reanalyze the experimental data of [2].

In principle, with all conventions carefully chosen, the formulas in the last two sections give the correct relative signs for the corrections with respect to the leading (potential model or SPA) amplitudes. For an independent check we combined our amplitudes (2.8) and (3.4) with the pure one-pion exchange bremsstrahlung amplitude [Fig. 1, diagram (a) with the internal  $\Delta$  line replaced by a nucleon line]. If the exchanged pion is numerically put on shell ( $q^0 \rightarrow \sqrt{\vec{q}^2 + m_\pi^2}$ ), this is equal up to a common factor to the pion-photoproduction amplitude with and without intermediate  $\Delta$  excitation. In a near-threshold geometry ( $\vec{q}^2 \sim 0$ ), the  $\Delta$  amplitude gives an enhancement of the cross section by a few percent, in agreement with Peccei's chirally invariant Lagrangian for  $\pi^0 p \rightarrow p\gamma$  [45] whereas the  $\omega/\rho$ -decay amplitudes interfere destructively, as in [24].

The sign of the  $\omega$ -coupling constant given in Eq. (3.7) is consistent with the pion-photoproduction data [24]. The sign of the much smaller radiative  $\rho$ -decay amplitude, however, is still the object of controversy [46]. We adopt here the sign convention of Gari and Hyuga [47] where the  $\rho$  decay enhances the contribution of the  $\omega$  decay in  $pp\gamma$ ; as the  $\rho$  contribution is only about 2% of the  $\omega$  (compare the respective coupling constants), a switch in the sign of  $g_{\rho\pi\gamma}$  would not alter our conclusions.

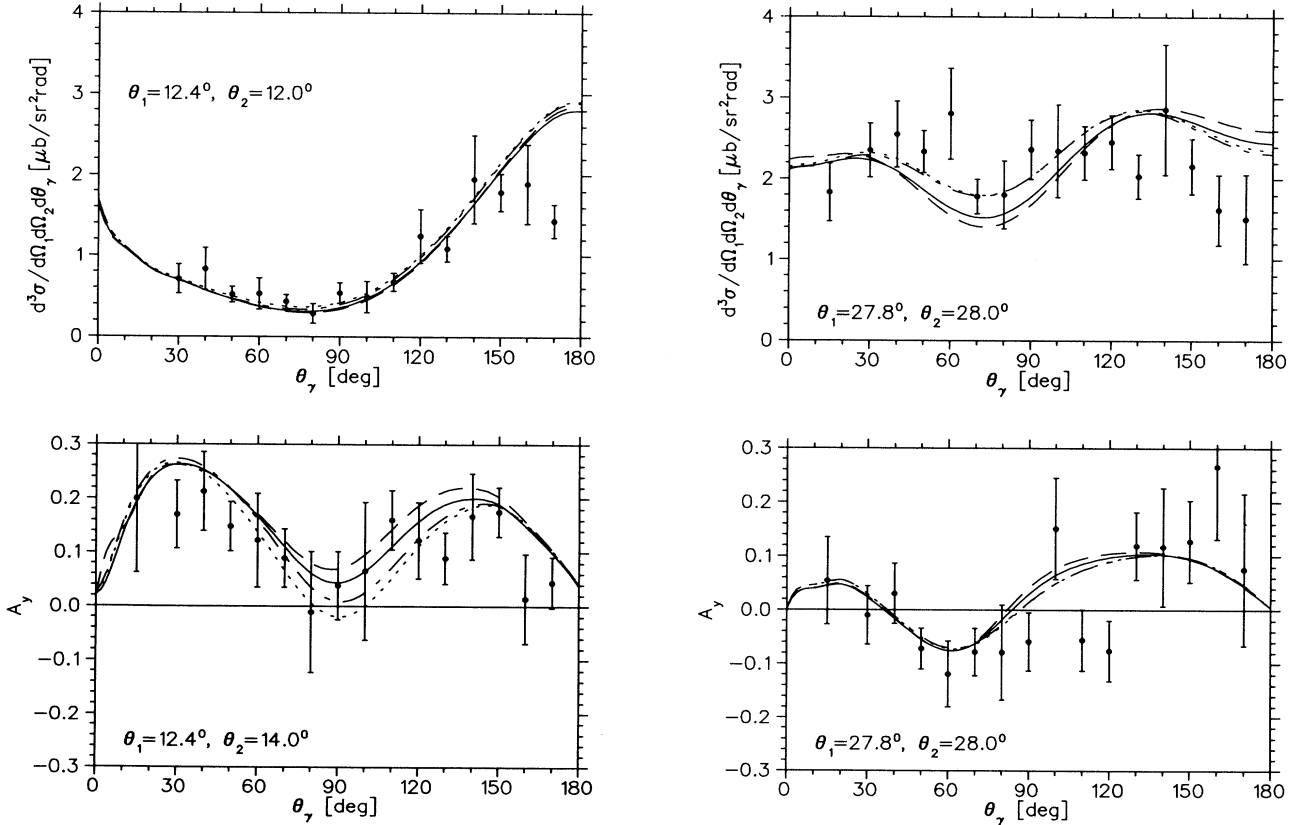


FIG. 2. Coplanar  $pp\gamma$  exclusive cross sections and analyzing powers at  $T_{\text{lab}} = 280 \text{ MeV}$  and for the smallest and largest proton angle pairs  $\theta_1, \theta_2$  of the TRIUMF experiment [3] (the data points shown are rescaled with a factor of 0.67 as in this reference). The curves denote the pure potential model of Ref. [6] (solid line), potential model plus pure  $\omega/\rho$  decay (long dashed line), and the full model according to models A (dotted lines) and B (dash-dotted line).

### A. Potential model results

All the calculations in this section are based on the inversion potential to the Nijmegen-II  $NN$  phase shifts used in Ref. [6]. Using another realistic  $NN$  potential would not change any of our results. The basic features of the potential model can be essentially represented in terms of two variables: the total energy of the process  $T_{\text{lab}}$  as a crucial parameter for the relative size of the various contributions in the amplitude and the opening angles of the two protons determining the maximum photon energy and thus the off-shell signature of the process [6]. The two examples of Fig. 2 show the coplanar, exclusive  $pp\gamma$  cross section  $d^3\sigma/d\Omega_1 d\Omega_2 d\theta_\gamma$  and the analyzing power  $A_y$  for the smallest and largest outgoing proton angle pairs measured in the  $T_{\text{lab}} = 280$  MeV TRIUMF experiment [3]. The plots show that both  $\Delta$  excitations and internal radiative decay contributions are small for the cross section at small proton angles as well as for the analyzing power  $A_y$  at large proton angles. The  $\Delta$

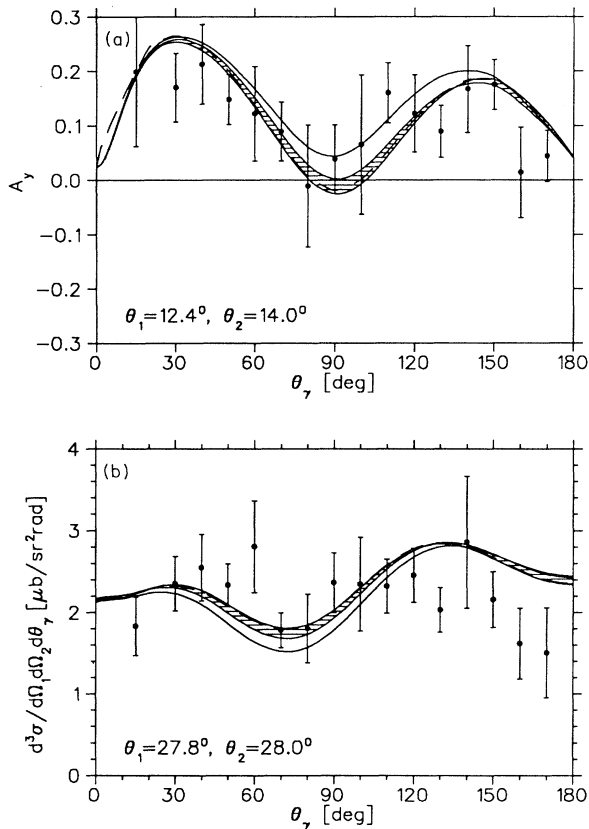


FIG. 3. Typical uncertainties of the  $\Delta$  contribution. The curves show the pure potential model of Ref. [6] (solid line) and the full calculation according to model A with standard parameters  $G_1 = 2.208$ ,  $G_2 = -0.278$ ,  $Z_\pi = Z_\gamma = -1/2$  (long dashed line). The upper bound of the shaded area in the cross section and lower bound in  $A_y$  correspond to larger electromagnetic couplings  $G_1 = 2.51$ ,  $G_2 = -1.62$ . The lower bound in the cross section and upper bound in  $A_y$  are calculated with larger  $Z$  parameters  $Z_\pi = Z_\gamma = -1/4$ .

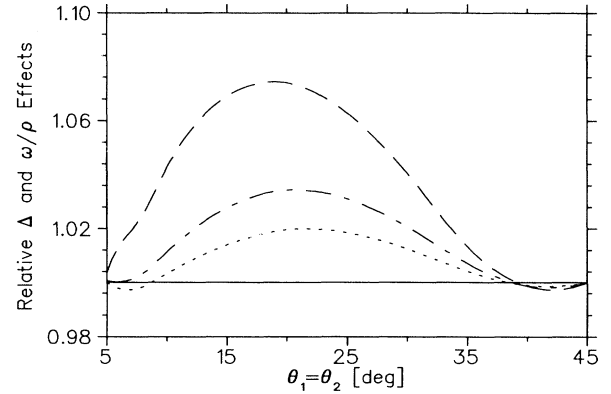


FIG. 4. Relative change of the integrated, coplanar  $pp\gamma$  cross section  $d^2\sigma/d\Omega_1 d\Omega_2$  (with corrections)/ $d^2\sigma/d\Omega_1 d\Omega_2$  (without corrections) at 280 MeV (dashed line), 200 MeV (dash-dotted line), and 157 MeV (dotted line) for parameter set A as a function of the symmetric proton angles  $\theta_1 = \theta_2$ .

contribution is the leading effect but tends to be partly canceled by the radiative decay contributions. The maximum net effect of both contributions can increase the differential cross section by (15–20)% at medium photon angles but amounts to only a few percent in the total cross section.

Among the examples of Fig. 2, only the  $12.4^\circ$ ,  $14^\circ$  analyzing power shows a sizable dependence on the parametrization of the  $\pi$  and  $\rho$  exchange. The choice of different electromagnetic couplings, e.g.,  $G_1 = 2.51$ ,  $G_2 = -1.62$ , hardly affects the  $\Delta$  contribution in the cross sections (Fig. 3). However, the choice of  $Z_\pi = Z_\gamma = -1/4$  [24] reduces the size of the  $\Delta$  contributions by roughly 20%. These two choices for the couplings and off-shell parameters are likely to be rather extreme. Moreover, because of its small relative size, a rescaling error in the  $\omega/\rho$  amplitude would not affect much the end results. As an example, the extreme case of no rescaling of this contribution at all would reproduce almost exactly the cross section and analyzing power results of the  $Z_\pi = Z_\gamma = -1/4$  case in Fig. 3. A shift in the  $\Delta$  mass due to self-energy insertions as given in [25] would reduce the  $\Delta$  contributions less strongly than the shift in the off-shell parameters. One might therefore conclude that the corrections are reasonably well determined in our model.

In order to obtain a more general picture we calculate the double differential cross section  $d\sigma/d\Omega_1 d\Omega_2 = \int d\theta_\gamma (d\sigma/d\Omega_1 d\Omega_2 d\theta_\gamma)$  and represent its relative enhancement due to the correction terms as a function of the symmetric angle  $\theta = \theta_1 = \theta_2$  (Fig. 4). Note that small  $\theta$  values correspond to a suppression of the meson four-momentum transfer ( $q \rightarrow 0$ ) whereas for large  $\theta$ , the elastic limit  $k \rightarrow 0$  is reached. In both cases, the amplitudes (2.8) and (3.4) are suppressed. They are maximum in the medium proton angle region  $\theta \sim 20^\circ$ . The relative size of the corrections dies down as the energy decreases and reaches only about 3% at  $T_{\text{lab}} = 200$  MeV.

In Fig. 5 the analysis of Fig. 2 is repeated for the

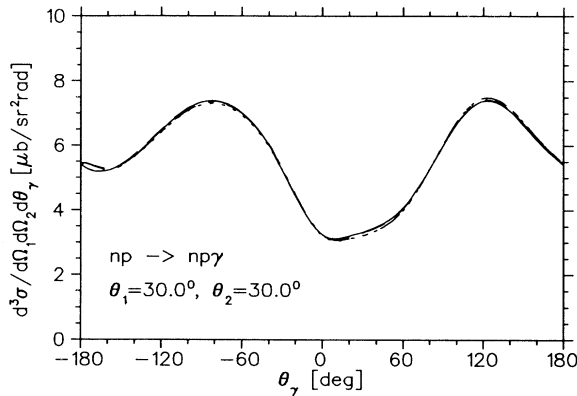


FIG. 5. Coplanar  $np\gamma$  exclusive cross section at  $T_{\text{lab}} = 280$  MeV. The curves denote the pure potential model of Ref. [6] (solid line), plus pure  $\omega/\rho$  decay (long dashed line), and the full model according to models A and B (dash-dotted and dotted lines).

$np\gamma$  observables. Here, the isospin factors yield strong destructive interference between the various Feynman graphs so that both the  $\Delta$  excitation and the radiative decays become negligible corrections to the potential model cross section. The same result holds for the  $np\gamma$ -analyzing power. We thus confirm the result of [15] that  $\Delta$  corrections to the  $np\gamma$  amplitude are weak.

### B. 730 MeV (SPA) results

Two typical geometries of the 730 MeV  $pp\gamma$  experiment reported in Ref. [44] are shown in Fig. 6. One proton is emitted at  $\theta_1 = 50.5^\circ$ ,  $\phi_1 = 0^\circ$  and the polar angles of the photon are  $\theta_\gamma = 67^\circ$ ,  $\phi_\gamma = 179^\circ$  for counter G7 and  $\theta_\gamma = 54^\circ$ ,  $\phi_\gamma = 131^\circ$  for counter G10. The solid curves have been obtained with the soft photon approximation of [43] averaged over the finite acceptance of the detector using the factors tabulated in Ref. [44]. Contributions in  $O(k)$  are only partly included in the SPA; the corrections considered here are thus specific candidates for the missing  $O(k)$  effects.

With the relatively high proton energy but  $k$  restricted by experimental constraints, the 730 MeV results are reasonably described for all but the largest  $k$  by the soft photon model that treats relativity and gauge invariance

correctly but omits higher order contributions in  $k$ . This can be seen from the complete set of results displayed in Ref. [44]. As expected our corrections are negligible for small  $k$  but increase with the photon energy. Analogous to the 280 MeV examples, there is a cancellation between the  $\Delta$  and  $\omega/\rho$  effects. The actual size is again geometry dependent but is limited to about 20% of the SPA cross section at  $k = 150$  MeV. A variation of the electromagnetic coupling constants and off-shell parameters within the experimental limits yields effects analogous to those shown in Fig. 3 and leaves a freedom of a few percent in our final  $k = 150$  MeV results. Correspondingly, the results are not much altered by interchange of models A and B. We conclude that a  $\Delta$  amplitude consistent with experimental results can only resolve a small part of the discrepancy between the SPA and the 730 MeV  $pp\gamma$  results at photon energies above  $\sim 100$  MeV.

### V. CONCLUDING REMARKS

We have evaluated the  $\Delta$  excitation and radiative  $\omega/\rho$  decay corrections to proton-proton and neutron-proton bremsstrahlung for the energy range up to  $T_{\text{lab}} \sim 1$  GeV. This was done by calculating the relativistic Born amplitudes and adding them to potential model and SPA amplitudes. The Born amplitudes were normalized by calculating  $\Delta$ -production and -absorption cross sections in the same model and fitting to experimental data and coupled channels predictions.

Of the two processes considered, the  $\Delta$  excitation dominates but is generally partly compensated by the radiative decay contributions. Both corrections together increase the 280 MeV  $pp\gamma$  integrated cross section  $d^2\sigma/d\Omega_1 d\Omega_2$  by an amount depending essentially on the proton opening angles  $\theta_i$  and reaching a maximum of roughly 7.5% at  $\theta_1 \sim \theta_2 \sim 20^\circ$ . The relative effect on  $d^3\sigma/d\Omega_1 d\Omega_2 d\theta_\gamma$  is maximum for photon emission around  $\theta_\gamma = 90^\circ$  and is typically  $\leq 20\%$ .

In the 730 MeV Rochester geometry, the corrections become relevant for photon energies above  $\sim 100$  MeV but are not large enough to complement the soft photon approximation and fit the experimental data [44].

We have taken care to study and discuss the limits and uncertainties of our model. The results have been obtained on the basis of two different parametrizations of the  $\Delta$  excitation (models A and B of Table I) but show little sensitivity to the underlying coupled channels model.

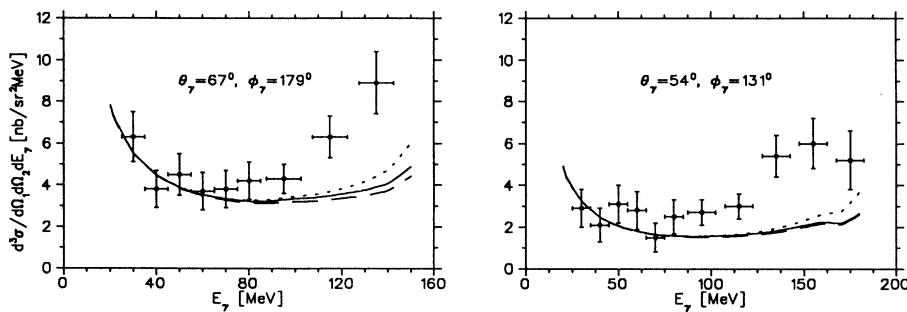


FIG. 6. 730 MeV  $pp\gamma$  measurements and soft photon approximation in two typical geometries (see [44] and text). The curves denote the pure SPA results (solid line), plus pure  $\omega/\rho$  decay (long dashed line), and the full model according to model A (dotted line).



The fact that the  $\Delta$ -excitation cross sections of models A and B are nearly identical, despite the rather massive differences in the values of the  $\rho$  couplings and the choice of form factors and propagators, is reassuring for our approach but corresponds to the result obtained earlier, that rather different potential models, once they fit the  $NN$ -scattering data, yield very similar bremsstrahlung results [6] and is disappointing if one hopes to understand the underlying physical reaction mechanism from  $NN\gamma$  measurements.

The experimental uncertainty in the radiative  $\Delta$ -decay constants and the off-shell freedom of the  $\Delta$  suggest a theoretical error of about  $\pm 20\%$  in the final correction amplitudes, i.e., up to  $\sim \pm 4\%$  in the total (280 MeV)  $pp\gamma$  cross section. We should mention that the discrepancies between the  $pp\gamma$  predictions of different  $NN$  potential models, which most bremsstrahlung experiments in the past were designed to isolate, are of the same order of magnitude. Given the present experimental status of nucleon-nucleon bremsstrahlung and the theoretical ambiguities mentioned, it is not possible to use  $NN\gamma$  data for putting limits on the parameters entering our correction amplitudes.

In view of the similarities of our calculation with previous *Ansätze*, a comprehensive comparison of the results seems worthwhile. First note that we have eliminated the uncertainty with respect to the relative sign of the relativistic corrections stated by Kamal and Szyjewicz [23] through a comparison with the pion-photoproduction process. Our  $\omega/\rho$ -decay amplitude extends the amplitude of [23] by including the  $\omega$ -tensor coupling terms

and the  $\rho$  decays and is, if we divide by  $g(T_{lab})$ , slightly smaller than given there.

The discrepancy of our result is more serious for the 730 MeV  $\Delta$ -excitation calculation where the previous authors lack a reliable model for the  $NN$ -channel  $pp\gamma$  amplitude. The authors of [17] therefore essentially fit the  $\Delta$ -excitation part to the experimental  $pp\gamma$  data. In [16], the suppression of the amplitude which we simulate by appropriate form factors is neglected. In both cases, the pure  $\Delta$  cross section becomes larger than ours by more than a factor of 10 and would be in clear contradiction to the 800 MeV  $\Delta$ -production data of, e.g., [26]. We also stress the importance of taking interference terms correctly into account.

The dispersion theoretic approach used in [15] to estimate the role of the  $\Delta$  resonance in a OPE  $np\gamma$  calculation is rather different from our model. Correspondingly, the results agree only in relative size.

Finally, a comparison with the coupled channels  $\Delta$  results of [18] in the low energy region shows good agreement for the cross sections and even for the analyzing powers  $A_y$ . This is encouraging for the feasibility of our method as well as for the various extensions made.

#### ACKNOWLEDGMENTS

We wish to thank Dr. S. Scherer for valuable discussions. This work was supported in part by a grant from the Natural Sciences and Engineering Research Council of Canada.

- 
- [1] C. A. Smith, J. V. Jovanovich, and L. G. Greeniaus, *Phys. Rev. C* **22**, 2287 (1980), and earlier publications quoted therein.
  - [2] B. M. K. Nefkens, O. R. Sander, and D. I. Sober, *Phys. Rev. Lett.* **38**, 876 (1977).
  - [3] K. Michaelian *et al.*, *Phys. Rev. D* **41**, 2689 (1990).
  - [4] P. Kitching *et al.*, *Phys. Rev. Lett.* **57**, 2363 (1986); *Nucl. Phys.* **A463**, 87 (1987).
  - [5] B. v. Przewoski *et al.*, *Phys. Rev. C* **45**, 2001 (1992).
  - [6] M. Jetter and H. V. von Geramb, *Phys. Rev. C* **49**, 1832 (1994). See also M. Jetter, H. Freitag, and H. V. von Geramb, *Nucl. Phys.* **A553**, 655c (1993); *Phys. Scr.* **48**, 228 (1993).
  - [7] R. L. Workman and H. W. Fearing, *Phys. Rev. C* **34**, 780 (1986).
  - [8] M. K. Liou and M. E. Sobel, *Ann. Phys. (N.Y.)* **72**, 323 (1972).
  - [9] K. Nakayama, *Phys. Rev. C* **39**, 1475 (1989).
  - [10] V. A. Herrmann and K. Nakayama, *Phys. Rev. C* **45**, 1450 (1992); V. Herrmann, J. Speth, and K. Nakayama, *ibid.* **43**, 394 (1991).
  - [11] V. Brown, P. L. Anthony, and J. Franklin, *Phys. Rev. C* **44**, 1296 (1991).
  - [12] A. Katsogiannis and K. Amos, *Phys. Rev. C* **47**, 1376 (1993).
  - [13] A. Katsogiannis, K. Amos, M. Jetter, and H. V. von Geramb, *Phys. Rev. C* **49**, 2342 (1994).
  - [14] V. R. Brown and J. Franklin, *Phys. Rev.* **8**, 1706 (1973).
  - [15] G. E. Bohannon, L. Heller, and R. H. Thompson, *Phys. Rev. C* **16**, 284 (1977).
  - [16] A. Szyjewicz and A. N. Kamal, in *Few Body Systems and Nuclear Forces I*, edited by H. Zingl, M. Haftel, and H. Zankel, *Lecture Notes in Physics*, Vol. 82 (Springer, Berlin, 1978); A. Szyjewicz and A. N. Kamal, in *Nucleon-Nucleon Interactions*, edited by D. Measday, H. Fearing, and A. Strathdee, *AIP Conf. Proc. No. 41* (AIP, New York, 1978), p. 502.
  - [17] L. Tiator, H. J. Weber, and D. Drechsel, *Nucl. Phys.* **A306**, 468 (1978).
  - [18] F. de Jong, K. Nakayama, V. Herrmann, and O. Scholten, *Phys. Lett. B* **333**, 1 (1994).
  - [19] J. A. Eden *et al.* (private communication) have recently performed a potential model calculation of  $\Delta$  effects in proton-proton bremsstrahlung.
  - [20] M. Schäfer *et al.*, *Nucl. Phys.* **A575**, 429 (1994).
  - [21] D. O. Riska, *Phys. Rep.* **181**, 207 (1989).
  - [22] Y. Ueda, *Phys. Rev.* **145**, 1214 (1966).
  - [23] A. N. Kamal and A. Szyjewicz, *Nucl. Phys.* **A285**, 397 (1977).
  - [24] H. Garcilazo and E. M. de Goya, *Nucl. Phys.* **A562**, 521 (1993).
  - [25] B. ter Haar and R. Malfiet, *Phys. Rep.* **149**, 208 (1987).
  - [26] J. Hudomalj-Gabitzsch *et al.*, *Phys. Rev. C* **6**, 2666 (1978).

- [27] V. Dmitriev, O. Sushkov, and C. Gaarde, Nucl. Phys. **A459**, 503 (1986).
- [28] R. Machleidt, in *Advances in Nuclear Physics*, edited by J. W. Negele and E. Vogt (Plenum, New York, 1989), Vol. 19.
- [29] J. D. Bjorken and S. D. Drell, *Relativistic Quantum Mechanics* (McGraw-Hill, New York, 1964).
- [30] R. Davidson, N. Mukhopadhyay, and R. Wittman, Phys. Rev. D **43**, 71 (1991).
- [31] S. Nozawa, B. Blankleider, and T.-S. H. Lee, Nucl. Phys. **A513**, 459 (1990).
- [32] R. Davidson, N. Mukhopadhyay, and R. Wittman, Phys. Rev. Lett. **56**, 804 (1986).
- [33] H. F. Jones and M. D. Scadron, Ann. Phys. (N.Y.) **81**, 1 (1973).
- [34] M. Warns *et al.*, Z. Phys. C **45**, 627 (1990).
- [35] R. H. Dalitz and D. G. Sutherland, Phys. Rev. **146**, 1180 (1966).
- [36] E. E. van Faassen and J. A. Tjon, Phys. Rev. C **28**, 2354 (1983).
- [37] E. E. van Faassen and J. A. Tjon, Phys. Rev. C **33**, 2105 (1986).
- [38] R. Wittman, Phys. Rev. C **37**, 2075 (1988).
- [39] M. G. Olsson and E. T. Osypowski, Nucl. Phys. **B87**, 399 (1975).
- [40] L. M. Nath and B. K. Bhattacharyya, Z. Phys. C **5**, 9 (1980).
- [41] L. M. Nath, B. Etemadi, and J. D. Kimel, Phys. Rev. D **3**, 2153 (1971).
- [42] Particle Data Group, K. Hikasa *et al.*, Phys. Rev. D **45**, S1 (1992).
- [43] H. W. Fearing, Phys. Rev. C **6**, 1136 (1972); H. W. Fearing, in *Nucleon-Nucleon Interactions*, edited by D. Measday, W. Fearing, and A. Strathdee, AIP Conf. Proc. No. 41 (AIP, New York, 1978), p. 506.
- [44] B. M. K. Nefkens, O. R. Sander, D. I. Sober, and H. W. Fearing, Phys. Rev. C **19**, 877 (1979).
- [45] R. D. Peccei, Phys. Rev. **181**, 1902 (1969).
- [46] P. Sarriguren, J. Martorell, and D. W. L. Sprung, Phys. Lett. B **228**, 285 (1989).
- [47] M. Gari and H. Hyuga, Nucl. Phys. **A264**, 409 (1976).